

strictly from the imagery was hampered by the broad, spectrally indistinct shape of the DE reflectance profile (Figure 3). DE appeared as an overall increase in pixel brightness, without a spectrally unique signature. Absolute concentration determination also was influenced by the reflectance of the bottom (background) signature, as can be seen on the lower left side of the imagery in Figure 1.

A modeling application of the hydrological studies software Delft3D-FLOW was undertaken in conjunction with the field experiment. Model results are highly dependent on vertical and horizontal mixing coefficients. The horizontal mixing coefficient was adjusted in order to establish reasonable agreement between the plume outlines derived from the imagery and the modeled plume at prescribed levels of dilution.

Normalizing the measured DE by the estimated near-field concentration implies a relative concentration of 0.38%. This compares well with the concentration predicted by the model at the point shown in Figure 2 (black triangle). Current speeds inferred from the imagery (45–63 centimeters per second) also closely agree with those derived from the model (40–60 centimeters per second). The plume thickness (approximately two meters) as inferred from the backscatter profile is similar to the estimated thickness developed within the model.

Final model adjustment activities will be undertaken using additional data collected from a 2006 field experiment. In 2006, the original experiment was expanded to include

the simultaneous release of a dye to test and evaluate the ability to track and model a plume with unique spectral characteristics. Data analysis is ongoing on the latter experiment. Together, these experiments will further the knowledge of the spatial, spectral, and temporal characteristics of plumes in coastal waters.

The plume experiments were conducted in conjunction with a Pacific Northwest National Laboratory (PNNL) field collection campaign in and around Sequim Bay on the Strait of Juan de Fuca. The objective of the field campaigns were to identify and characterize features in the nearshore environment from the standpoint of quantifying environmental parameters to improve operational planning for applications such as coastal zone management.

This field collection campaign provided a unique opportunity for a multisensor data collection effort in littoral regions, in order to identify and characterize features from multiple platforms (satellite, aerial, water surface, and subsurface) and sensors. Data from this mission are being used as input to both radiative transfer and ocean transport models, for characterizing the water column and the near shore, and for quantitatively estimating circulation and transport in coastal environments.

Research and development activities are ongoing; a 2006 follow-on experiment was conducted to collect additional data to refine model calibration and validation. The 2006 campaign compiled additional data to refine and improve the modeling results for char-

acterizing the spatial and spectral characteristics of a man-made plume in coastal waters. Such experiments will help refine future models for operational planning and coastal zone management in this and other areas.

Acknowledgments

The authors thank and acknowledge the support from the U.S. Office of Naval Research under Interagency Agreement N00014051P2 0087F.

References

- Carder, K. L., and R. G. Steward (1985), A remote-sensing reflectance model of a red-tide dinoflagellate off west Florida, *Limnol. Oceanogr.*, 30(2), 286–298.
- Davis, C. O., J. Bowles, R. A. Leathers, D. Korwan, T. V. Downes, W. A. Snyder, and W. Chen (2002), Ocean PHILLS hyperspectral imager: Design, characterization, and calibration, *Opt. Express*, 10(4), 12 pp.

Author Information

Karen L. Steinmaus, Marine Sciences Laboratory, Pacific Northwest National Laboratory (PNNL), Sequim, Wash.; currently at the International Atomic Energy Agency, Vienna, Austria; E-mail: k.steinmaus@iaea.org; Jeffery Bowles, Remote Sensing Division, Ocean and Atmospheric Science and Technology Branch, Naval Research Laboratory, Washington D.C.; Dana Woodruff, Marine Sciences Laboratory, PNNL; Timothy Donato, William J. Rhea, William Snyder, and Dan Korwan, Remote Sensing Division, Ocean and Atmospheric Science and Technology Branch, Naval Research Laboratory; Lee Miller, Greg Petrie, Adam R. Maxwell, and Lyle Hibler, Marine Sciences Laboratory, PNNL.

Monitoring Anak Krakatau Volcano in Indonesia

PAGES 581, 585–586

Krakatau volcano, in Indonesia, showed its destructive vigor when it exploded in 1883 [*Self and Rampino*, 1981]. The eruption and subsequent tsunamis caused more than 35,000 casualties along the coasts of the Sunda Strait. In 1928, the 'child' of Krakatau, Anak Krakatau, emerged from the sea at the same location as its predecessor and has since grown to a height of 315 meters (Figure 1a). The volcano exhibits frequent activity—on average one large eruption every four years—yet again posing risk for the coastal population of Java and Sumatra and for the economically important shipping routes through the Sunda Strait.

Following the active phase of Anak Krakatau in 1980, the Center for Volcanology and Geological Hazard Mitigation (CVGHM) within the Geological Agency of Indonesia established a permanent volcano observatory on the western coast of Java in Pasauran, about

50 kilometers east of the Krakatau archipelago. The two-member staff monitors the activity of Anak Krakatau on a 12-hour heliograph, which is connected to a short-period seismometer on the volcano's flank, and by visual control (when weather allows). The daily seismic event statistics are radioed to the CVGHM headquarters in Bandung. They are used to determine the current alert level, on the basis of which Indonesian authorities decide about preventive measures. By these means, tourism around the archipelago was prohibited twice, in April and May 2005, due to an increase in seismicity. The joint Indonesian-German Krakmon Project was developed to improve early warning procedures for volcano-induced risks in the Sunda Strait and the adjacent densely populated coasts of Java and Sumatra.

Project Aims and Setting

The project's backbone is the development of a permanent multiparameter monitoring system for Anak Krakatau. Its main purpose is to automatically quantify the activity status

of the volcano based primarily on the recorded seismicity. However, the multiparameter approach allows researchers to investigate correlations among different geophysical, geochemical, and environmental parameters and to deduce cause-and-effect relationships.

Anak Krakatau is one of the fastest growing volcanoes on Earth and provides the opportunity to study volcanic processes throughout different episodes of activity. This improves the understanding of dynamic processes inside volcanoes and of external forcing that may influence their activity. Only by knowing the characteristic behavior of specific volcanoes can science provide valuable information for efficient risk mitigation procedures.

Krakatau volcano erupts material of a wider compositional range compared with other volcanoes of the Sunda Arc subduction system [*Harjono et al.*, 1989]. This is due to its location within the Sunda Strait (Figure 1c), which represents an extensional hinge-line accommodating the clockwise rotation of Sumatra relative to Java and the northward displacement of the Sumatra forearc sliver along the Great Sumatra Fault [e.g., *Schlüter et al.*, 2002]. Quaternary volcanic edifices align along a lineament that trends perpendicular to the trench. Therefore, it can be assumed that the tectonic regime responsible for triggering volcanic activity is not controlled purely by subduction processes.

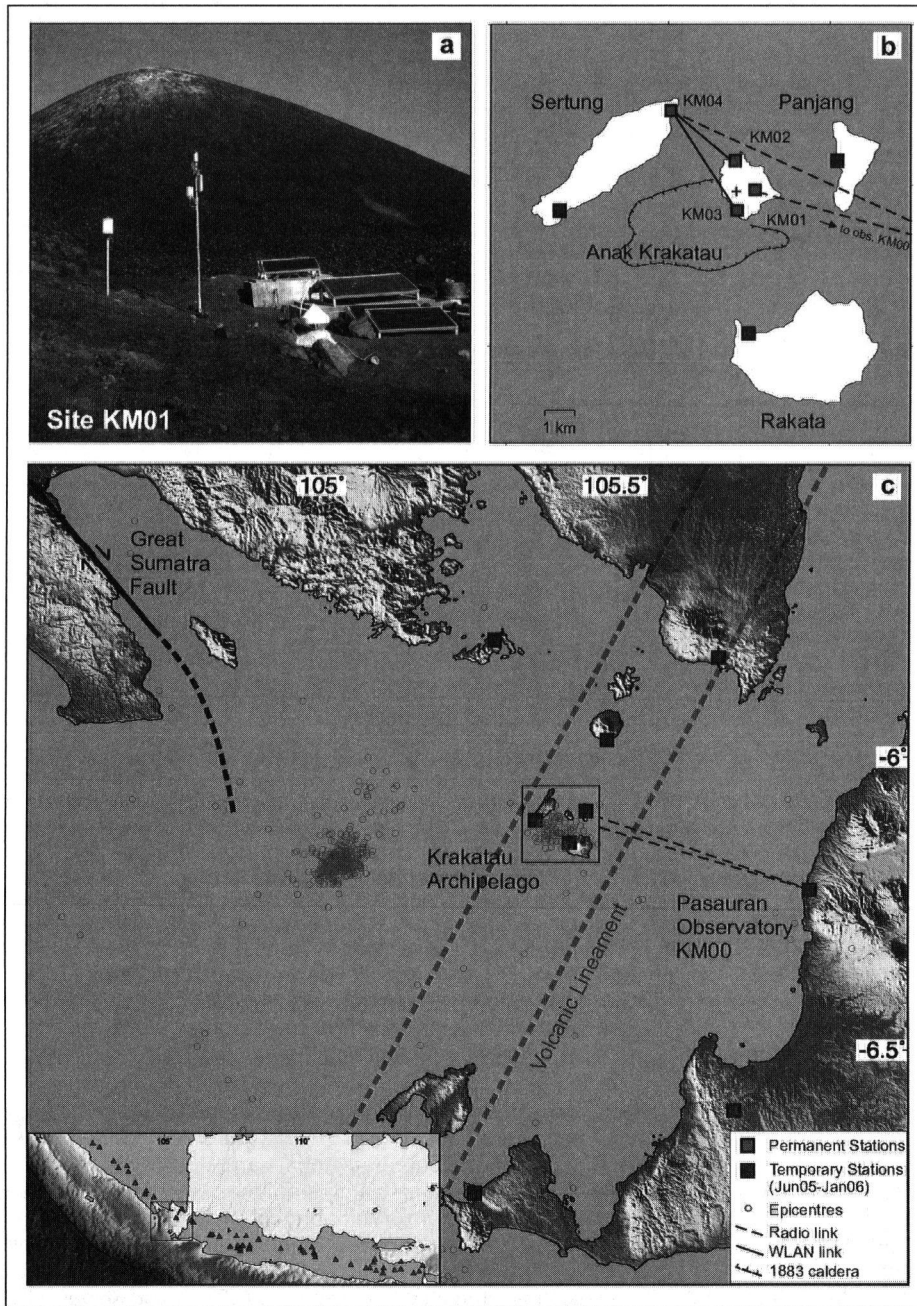


Fig. 1. (a) Main monitoring site with vaults for seismic and gas equipment, located below Anak Krakatau's summit. (b) Network of monitoring stations on the Krakatau archipelago. (c) Location of Krakatau within the Sunda Strait. Red circles are preliminarily located epicenters of approximately 800 earthquakes recorded during eight months using stations of the permanent and temporary networks. The inset is the location of the Sunda Strait with respect to Indonesia's Sumatra and Java Islands. Original color image appears at the back of this volume.

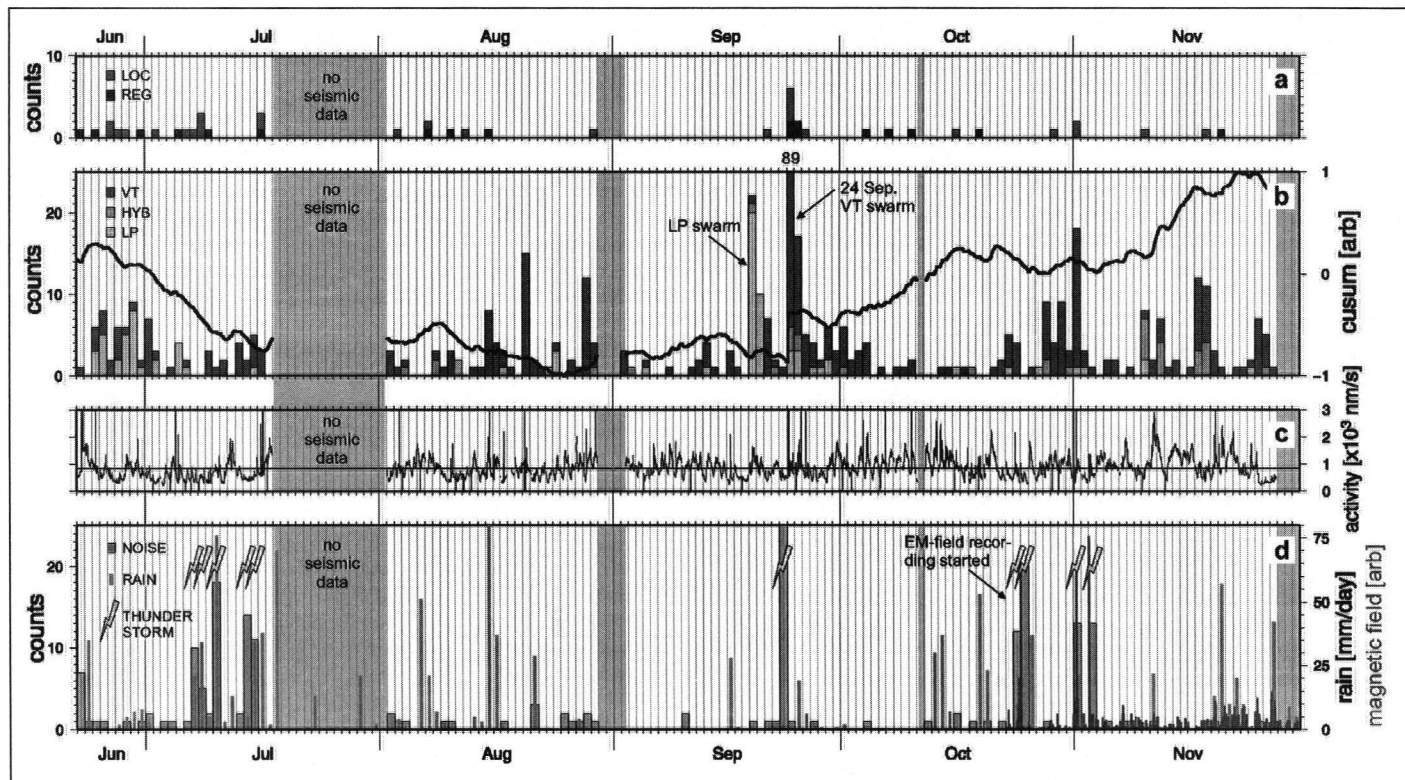


Fig. 2. Statistics of automatically detected event types, seismic activity, and magnetic and meteorological data recorded on Anak Krakatau from June to November 2005. (a) Local (LOC) and regional (REG) event counts. (b) Volcano-related event counts. VT, volcano-tectonic; HYB, hybrid; LP, long-period. The black curve (cusum) shows the cumulative sum of differences calculated from the activity curve. (c) Absolute value of seismic amplitude averaged over 10-minute time windows for station KM01 (activity). The horizontal black line gives the mean used as reference value to calculate the cusum curve in Figure 2b. (d) Counts of transient seismic noise signals (grey), local rainfall (blue), magnetic field (high-pass-filtered and rectified, red), and thunderstorms observed (yellow). Note that increased noise signal counts highly correlate with the occurrence of thunderstorms. Original color image appears at the back of this volume.

Monitoring System

The monitoring system on Anak Krakatau is designed for long-term continuous and simultaneous recording of geophysical, environmental, and gas-geochemical data (Table 1). Three sites are arranged around the active cone (Figure 1b), each of which is equipped with a seismometer and a GPS sensor. Station KM01 is located closest to the crater on an old caldera rim. It connects to a gas monitoring system via radio link. Electromagnetic sensors are installed at station KM05, a few hundred meters away from station KM01, and connected to the latter via wireless local-area network (WLAN). Stations KM02 and KM03 are WLAN-linked to site KM04 on the island of Sertung that also hosts another seismometer and a surveillance camera. The data acquisition center in Pasauran on Java (KM00) receives the data streams via radio links (Figure 1).

The observatory is integrated into the German Indonesian Tsunami Early Warning System (GITEWS; <http://www.gitews.org/>), and data is accessible via Internet through a satellite connection. In addition to the permanently installed instruments on Krakatau, a temporary network of nine seismic stations was deployed in the Sunda Strait region and operated for eight months (Figure 1c).

A detector algorithm processes the incoming stream of seismic data from station

KM01. Using an artificial neural network approach, detected events automatically are classified based on several parameters extracted from the waveforms (e.g., duration, impulsiveness) and corresponding spectrums (e.g., dominant frequencies). This way, there is a differentiation between regional earthquakes (REG, originating mainly from the Sunda Arc subduction zone) and local earthquakes (LOC, epicenters within Sunda Strait but outside the Krakatau archipelago), and volcano-tectonic (VT), long-period (LP), and hybrid-type (HYB) events. Furthermore, transient noise signals are detected.

Since the Krakatau islands are not inhabited, human-made noise is very limited. Most of the noise signals recorded are from tropical thunderstorms coupled into the solid ground. This could be verified using records of the meteorological and electromagnetic sensors installed on the volcano (Figure 2d), as well as by visual and acoustic observations. The neural-network-based identification of event types proved to be stable; numerous tests established that the network outputs are highly reliable.

The classification of events is used for measuring the activity of the volcano based on daily event statistics (Figure 2). The automatic system drastically reduces the event counts compared with the visual analysis of the analogue records. This is due mainly to better recognition of transient

noise. These signals produce waveforms, which, on the analogue records, are hard to distinguish from those produced by volcanic sources.

In addition to the event-based activity measurement, several methods to break down the seismic data to a single value, which can be used as a proxy for the volcano's state of activity, have been tested. Among these are the calculation of (real-time) seismic amplitude and seismic spectrum [e.g., *Endo and Murray*, 1991], trend analysis [e.g., *Aspinall et al.*, 2006], and the determination of a base level noise seismic spectrum as suggested by *Vila et al.* [2006].

Seismicity Characteristics and Activity Status

Within the ongoing low-activity phase of Anak Krakatau, only a few events per day (commonly less than 15) occur that can be attributed to originate within the volcanic system (VT, HYB, LP; Figure 2b). However, phases of significantly increased seismic activity also are observed. A swarm of VT-type events occurred on 24 September 2005 and lasted until the beginning of October. The epicenters of the swarm cluster within the archipelago in the region of the old Krakatau Caldera (Figures 1c and 2b).

Interestingly, a swarm of LP events that may indicate a change in the magmatic

conduit system was recorded several days prior to the VT activity (Figure 2b). However, whether these two occurrences are linked remains speculative. The composition of fumarolic gases, for example, has not changed following the LP activity. Another earthquake swarm occurred in January 2006 about 25 kilometers farther to the west (Figure 1c). It is not yet known if this focused seismic activity is connected with larger-scale tectonic features such as the Great Sumatra Fault or even with new volcanic activity. Note that volcanic tremor has not been recorded since the installation of instruments.

Each spike in the seismic activity curve for station KM01 depicts a stronger earthquake that is reflected either in the counts of volcanic sources or in the REG/LOC counts (Figure 2c). A trend toward increasing or decreasing activity is not immediately evident for the time span shown. In comparison, a plot of the cumulative sum of differences (cusum) with respect to the mean value of activity depicts trends more clearly (Figure 2b) [Aspinall *et al.*, 2006]. Note that strong earthquakes cause a 'step,' or sudden increase in value, in the cusum curve, as can be seen at the beginning of the 24 September VT swarm.

While event count statistics describe the occurrence of transient seismic signals only, the activity and cusum curves bear additional information on the amplitudes of continuous signals, such as the background seismic noise. The level of background noise can be a good indicator of the volcano's state of activity [e.g., Vila *et al.*, 2006]. However, meteorological factors such as wind and rain also contribute to the noise levels recorded. For time spans in which cusum and event statistic strongly diverge, a strong, though nonlinear, correlation with meteorological phenomena could be seen. One of the future tasks will be to develop a data processing scheme that removes these influences from the data in order to reveal seismic noise levels that are related to volcanic sources solely.

It has to be emphasized that the data shown in Figure 2 reflect a phase of relative rest of Anak Krakatau. An increase in activity and the occurrence of new signals, such as volcanic tremor, will indicate whether the algorithms applied for the event detection and the tested parameterization schemes for volcanic activity are appropriate to define thresholds that aid or even automate alert-level assignment. Although installations and the implementation of all parameters into the monitoring procedure are not yet completed, the experience gathered so far by project scientists using this system has been very promising. The monitoring system has the potential to reveal comprehensive infor-

Data Type	Parameter	Instrumentation	Sampling Rate	Protocol ¹	Site KM
Geophysical	Seismicity	Broadband seismometer (STS2)	100 hertz (Hz)	RTP ²	01, 04
		Short-period seismometer (LE-3D)	100 Hz	RTP ²	02, 03
		Accelerometer (PA-23)	100 Hz	RTP ²	01
	Deformation	Novatel GPS	15 seconds	TCP ³	00, 01, 02, 03
	Electromagnetics	Fluxgate magnetometer, non-polarizing electrodes	100 Hz	RTP ²	05
	Soil temperature	Thermo-couple	1 Hz	RTP ²	01, 02, 05
Environmental	Weather	Rain Gauge, Thermohygrometer, 2D-Anemometer, Barometer	10 seconds	FTP ⁴	01
	Sea level	Tide gauge	1 Hz	RTP ²	02
	Video	1 Megapixel camera	variable (1 picture/hour)	FTP ⁴	04
Geochemical	Fumarolic Gases	Sensors: CO ₂ , SO ₂ , H ₂ S, (flow, concentration), gas temperature	10 seconds	TCP ³	01

¹ protocol used for data transfer to Pasauran Observatory Data Centre

² Reftek Transfer Protocol. Data archived in miniseed format.

³ Transmission Control Protocol.

⁴ File Transfer Protocol

mation on physical processes within Krakatau volcano. Reliable activity status estimates will significantly improve alerting procedures for this volcano.

Acknowledgments

Krakmon is a subproject of the Sundaarc initiative, funded by the German Federal Ministry of Education and Research (BMBF) and the Deutsche Forschungsgemeinschaft (DFG) within the framework of the geoscientific research and development program Geotechnologien (FKZ03G0578A; <http://www.geotechnologien.de/>). We are grateful for the help and hard work of Hendra Gunawan, Michael Lindemann, Jürgen Poggenburg, Hanno Schmidt, and Ahmad Solikhin.

References

Aspinall, W.P., R. Carniel, O. Jaquet, G. Woo, and T. Hicks (2006), Using hidden multi-state Markov models with multi-parameter volcanic data to provide empirical evidence for alert level decision-support, *J. Volcanol. Geotherm. Res.*, 153, 112–124.

Endo, E. T., and T. Murray (1991), Real-time Seismic Amplitude Measurements (RSAM): A volcano

monitoring and prediction tool, *Bull. Volcanol.*, 53, 533–545.

Harjono, H., M. Diament, L. Nouaili, and J. Dubois (1989), Detection of magma bodies beneath Krakatau volcano (Indonesia) from anomalous shear waves, *J. Volcanol. Geotherm. Res.*, 39, 335–348.

Schlüter, H. U., C. Gaedicke, H. A. Roeser, B. Schreck- enberger, H. Meyer, and C. Reichert (2002), Tectonic features of the southern Sumatra–western Java forearc of Indonesia, *Tectonics*, 21(5), 1047, doi:10.1029/2001TC901048.

Self, S., and M. R. Rampino (1981), The 1883 eruption of Krakatau, *Nature*, 294, 699–704.

Vila, J., R. Macia, D. Kumar, R. Ortiz, H. Moreno, and A. M. Correig (2006), Analysis of the unrest of active volcanoes using variations of the base level noise seismic spectrum, *J. Volcanol. Geotherm. Res.*, 39, 11–20.

Author Information

Arne Hoffmann-Rothe, Malte Ibs-von Seht, Rudolf Knieß, Eckhard Faber, Klaus Klinge, and Christian Reichert, Federal Institute for Geosciences and Natural Resources, Hanover, Germany; E-mail: a.hoffmann-rothe@bgr.de; Mas Atje Purbawinata and Cahya Patria, Center for Volcanology and Geological Hazard Mitigation, Bandung, Indonesia.

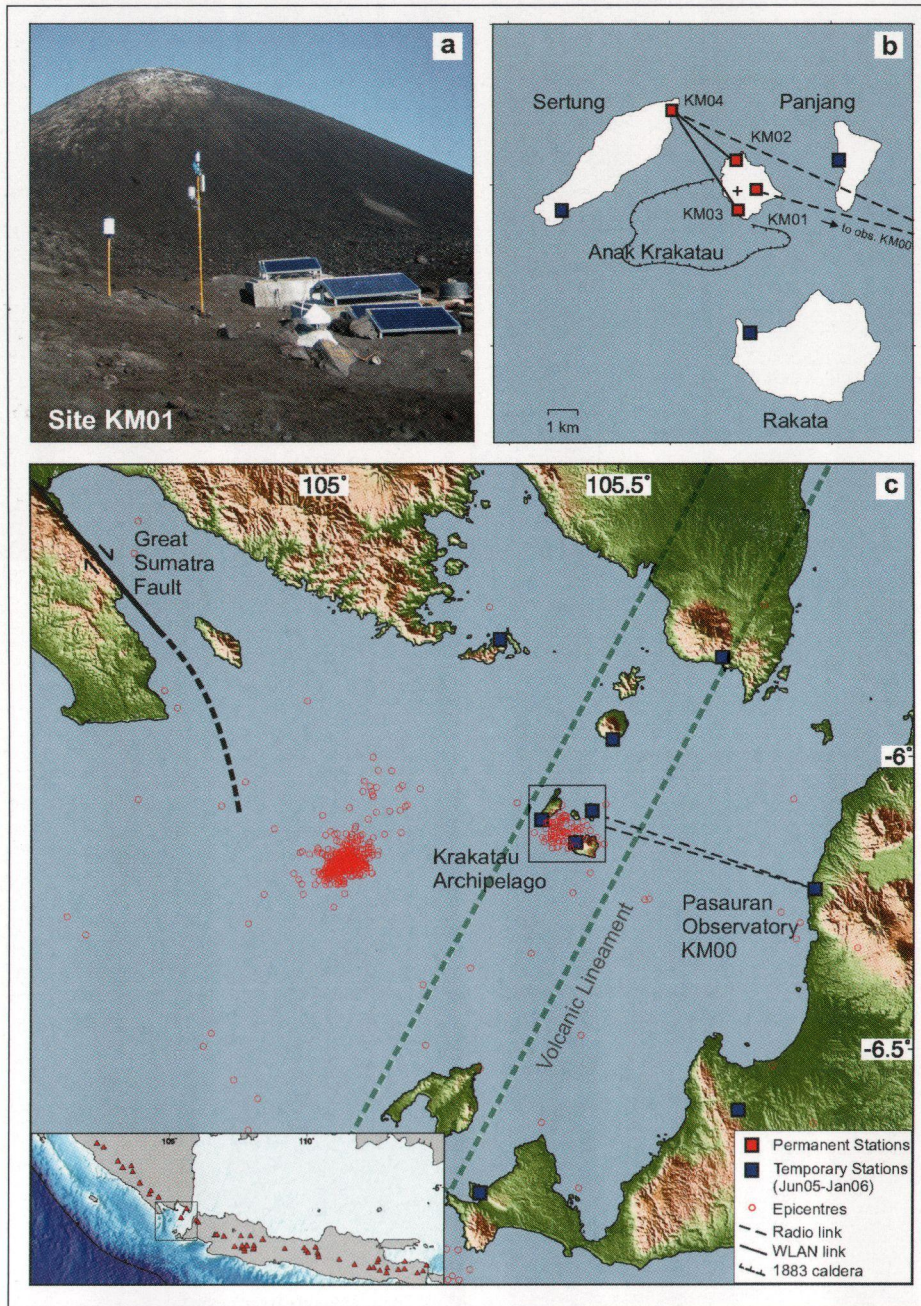


Fig. 1. (a) Main monitoring site with vaults for seismic and gas equipment, located below Anak Krakatau's summit. (b) Network of monitoring stations on the Krakatau archipelago. (c) Location of Krakatau within the Sunda Strait. Red circles are preliminarily located epicenters of approximately 800 earthquakes recorded during eight months using stations of the permanent and temporary networks. The inset is the location of the Sunda Strait with respect to Indonesia's Sumatra and Java Islands.

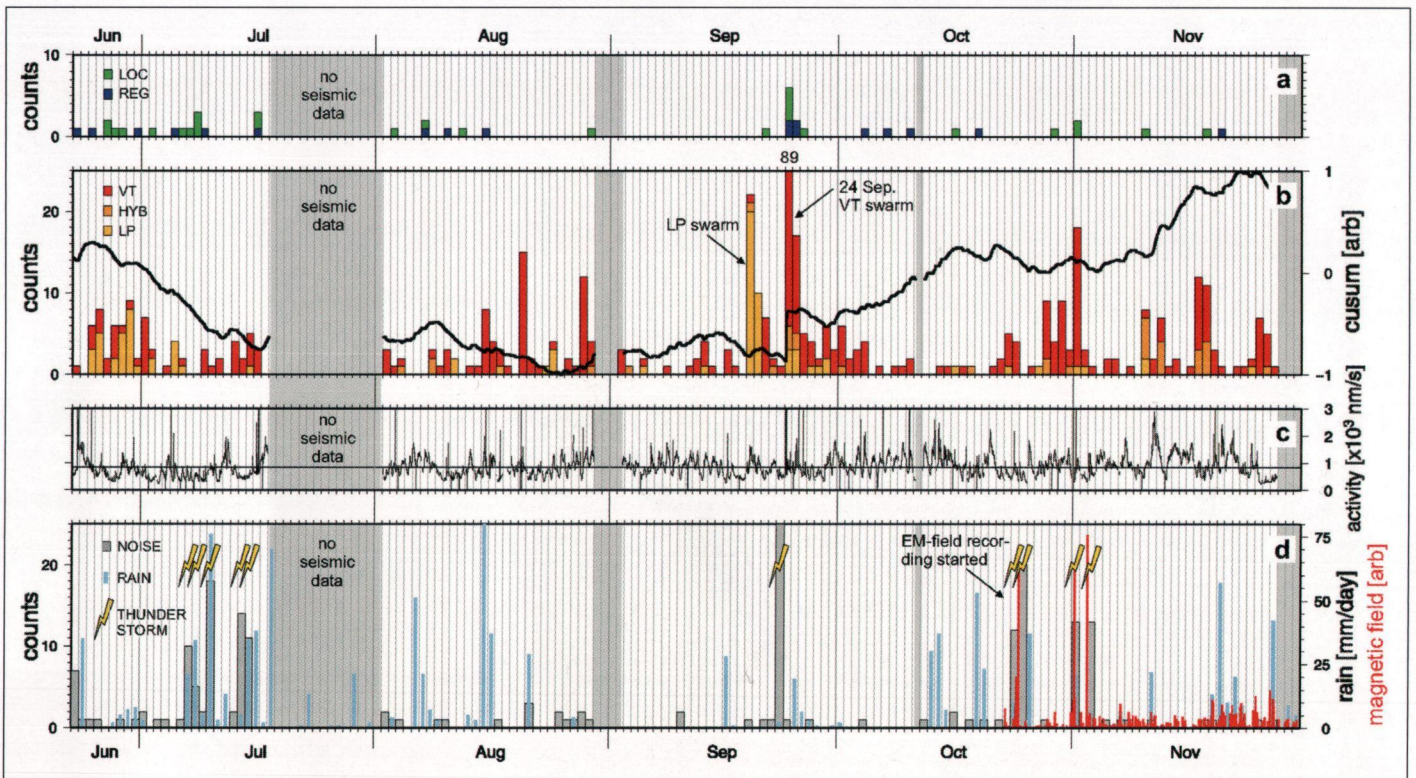


Fig. 2. Statistics of automatically detected event types, seismic activity, and magnetic and meteorological data recorded on Anak Krakatau from June to November 2005. (a) Local (LOC) and regional (REG) event counts. (b) Volcano-related event counts. VT, volcano-tectonic; HYB, hybrid; LP, long-period. The black curve (cusum) shows the cumulative sum of differences calculated from the activity curve. (c) Absolute value of seismic amplitude averaged over 10-minute time windows for station KM01 (activity). The horizontal black line gives the mean used as reference value to calculate the cusum curve in Figure 2b. (d) Counts of transient seismic noise signals (grey), local rainfall (blue), magnetic field (high-pass-filtered and rectified, red), and thunderstorms observed (yellow). Note that increased noise signal counts highly correlate with the occurrence of thunderstorms.